Accepted Manuscript

A novel class of α-glucosidase and HMG-CoA reductase inhibitors from *Ganoderma leucocontextum* and the anti-diabetic properties of ganomycin I in KK-A^{y} mice

Kai Wang, Li Bao, Ke Ma, Jinjin Zhang, Baosong Chen, Junjie Han, Jinwei Ren, Huajun Luo, Hongwei Liu

PII: S0223-5234(16)30953-9

DOI: 10.1016/j.ejmech.2016.11.015

Reference: EJMECH 9048

To appear in: *European Journal of Medicinal Chemistry*

Received Date: 30 July 2016

Revised Date: 12 October 2016

Accepted Date: 7 November 2016

Please cite this article as: K. Wang, L. Bao, K. Ma, J. Zhang, B. Chen, J. Han, J. Ren, H. Luo, H. Liu, A novel class of α-glucosidase and HMG-CoA reductase inhibitors from *Ganoderma leucocontextum* and the anti-diabetic properties of ganomycin I in KK-A^{y} mice, *European Journal of Medicinal Chemistry* (2016), doi: 10.1016/j.ejmech.2016.11.015.

A novel class of α- glucosidase and HMG-CoA reductase inhibitors from *Ganoderma leucocontextum* and the anti-diabetic properties of ganomycin I in KK-A^y mice

Kai Wang, [†,‡,⊥] Li Bao, [†,⊥] Ke Ma, [†,‡] Jinjin Zhang, [†,‡] Baosong Chen, [†,‡] Junjie Han, [†] Jinwei Ren, [†] Huajun Luo, [§] Hongwei Liu [†,‡,*]

[†] *State Key Laboratory of Mycology, Institute of Microbiology, Chinese Academy of Sciences, No.1 Beichenxi Road, Chaoyang District, Beijing 100101, P. R. China*

[‡] *Cunji Collage of Medicine, University of Chinese Academy of Sciences, Beijing, 100049, P. R. China*

[§] *Hubei Key Laboratory of Natural Products Research and Development, College of Biological and Pharmaceutical Science, China Three Gorges University, Yichang, 443002, P. R. China*

[†]Institute of Microbiology.

[‡] University of Chinese Academy of Sciences.

[§] *China Three Gorges University, Yichang, 443002, P. R. China*

[⊥]K. Wang, L. Bao contributed equally to this article.

* Corresponding Author Tel: +86 10 64806076; E-mail: liuhw@im.ac.cn (H-W, Liu)

Abstract

Three new meroterpenoids, ganoleucin A–C (**1**–**3**), together with five known meroterpenoids (**4**–**8**), were isolated from the fruiting bodies of *Ganoderma leucocontextum*. The structures of the new compounds were elucidated by extensive spectroscopic analysis, circular dichroism (CD) spectroscopy, and chemical transformation. The inhibitory effects of **1**-**8** on HMG-CoA reductase and α-glucosidase were tested *in vitro*. Ganomycin I (**4**), **5**, and **8** showed stronger inhibitory activity against HMG-CoA reductase than the positive control atorvastatin. Compounds **1**, and **3-8** presented potent noncompetitive inhibitory activity against α-glucosidase from both yeast and rat small intestinal mucosa. Ganomycin I (**4**), the most potent inhibitor against both *α*-glucosidase and HMG-CoA reductase, was synthesized and evaluated for its *in vivo* bioactivity. Pharmacological results showed that ganomycin I (**4**) exerted potent and efficacious hypoglycemic, hypolipidemic, and insulin-sensitizing effects in KK-A^y mice.

Keywords: *Ganoderma leucocontextum*, Meroterpenes, HMG-CoA reductase inhibition, α-Glucosidase inhibition, Anti-diabetic activities

Abbreviations: CD, circular dichroism; HMG-CoA reductase, 3-hydroxy-3-methylglutaryl co-enzyme A reductase; AUC, Area Under the Curve; OSTT, oral sucrose tolerance test; ISI, insulin sensitivity index; OGTT, oral glucose tolerance test; ITT, insulin tolerance test; NEFA, non-esterified fatty acid; TG, triglyceride; TC, Total Cholesterol; LDL-C, Low Density Lipoprotein-Cholesterol; HDL, High Density Lipoprotein-Cholesterol; AST, Aspartate Aminotransferase; ALT, Alanine transaminase

1. Introduction

Diabetes mellitus and the interrelated disorders of the metabolic syndrome have become an epidemic and worldwide public health issue [1,2]. Metabolic syndrome is characterized by insulin resistance, central obesity, elevated blood pressure, and dyslipidemia [3]. The current clinical drugs for the treatment of diabetes and metabolic syndrome (e.g. insulin, metfolin, statins, fibrates, and angiotensin-converting enzyme inhibitors) are still facing some problems due to the limitation of the therapeutic efficacy and the accompanying side effects [4,5]. Much effort has been made to develop a new drug that can ameliorate the metabolism of both glucose and lipids without side effects in the pharmaceutical industry.

Ganoderma species (Ganodermataceae, Polyporales) are well-known as elixir in China, and being widely used as functional foods and traditional medicine in Asian country [6]. Recently, a great deal of work has been carried out on this fungus, indicating that some ingredients from *Ganoderma* species have hypoglycemic and hypolipidemic [7-10]; The mushrooms of Ganoderma were reported to contain lanostane triterpenes, meroterpenes, alkaloids, and polysaccharides as bioactive constituents [11,12].In our continuous research on bioactive components from Ganoderma species, sixteen new triterpenes with inhibitory effects on HMG-CoA reductase and α-glucosidase were isolated from the fruiting of *G. leucocontextum* [13]. Further chemical investigation on this mushroom led to the isolation of eight meroterpenes including three new compounds (**1**-**3**). In recent years, a number of new meroterpenes with unusual skeletons and interesting bioactivities were reported from *Ganoderma* species. These *ganoderma*-derived meroterpenes presented various bioactivities including renoprotective activity [14], anti-fibrotic activity [15], anti-allergic activity [16], anti-HIV activity [17], and inhibitory activities against monocyte chemotactic protein 1(MCP-1) [18], p-Smad3 [19], acetylcholinesterase (AChE) [20], and $Ca_v3.1$ type calcium channel (TTCC) [21]. Herein, we would like to describe the isolation, structure determination, *in vitro* bioactivities of **1**-**8**, and the *in vivo* anti-diabetic effect of ganomycin I (**4**).

2. Results and discussion

*2.1 Isolation and structure elucidation of compounds **1**-**8**.*

The ethanol extract of *G. leucocontexum* was partitioned between water and ethyl acetate. The ethyl acetate-soluble fraction was subjected to chromatographic

separation using silica gel, ODS, Sephadex LH-20, and preparative HPLC to yield 8 meroterpenoids **1**-**8**. Five known compounds (**4**−**8**) were identified as ganomycin I (**4**) [18], ganomycin B (**5**) [23], fornicin C (**6**) [24], fornicin B (**7**) [24], and ganomycin C (**8**) [25] by comparison of their spectroscopic data with the literature data. (Supporting information Table S1)

Compound **1** was obtained as a colorless oil. Its molecular formula was assigned to be $C_{21}H_{28}O_5$ from its HRTOFMS at m/z 361.2011 $[M+H]^+$ and NMR data (8 degrees of unsaturation) (Table 1). The 1H NMR spectrum of 1 contains a typical ABX spin system [δH 6.87 (1H, d, *J* = 2.9 Hz), 6.75 (1H, dd, *J* = 8.8, 2.9 Hz), 6.72 (1H, d, *J* = 8.8 Hz)], suggesting the presence of a 1, 2, 4-trisubstitued benzene ring, two olefinic protons [δH 6.19 (1H, t, *J* = 7.3 Hz), 5.14 (1H, t, *J* = 7.2)], one oxygenated methane [δH 3.73 (1H, t, *J* = 9.0 Hz)], and three methyl groups [δH 1.52 (1H, s), 1.34 (1H, s), 1.05 (1H, s)]. Analysis of its ^{13}C NMR (Table 1) showed 21 carbon resonances, including three methyls, five methylenes, six methines (four olefinic, and one oxygenated), and seven quaternary carbons (one carbonyl, five olefinic, and one ketal). The NMR data of **1** were similar to those of compound **5**, except for two oxygenated carbons at δc 71.4 (C-10) and δc 83.0 (C-11) instead of two olefinic carbons. The above NMR evidence revealed a skeleton of prenylated hydroquinone. The HMBC (Fig. 2) correlations from H-10 [δ_H 3.73 (t, *J* = 9.0 Hz)] to C-8 (δ_c 35.8), C-9 (δ_c 27.8), C-11(δ_c 83.0), C-12, and C-13, and from H_3-12 (13) [δ_H 1.05 (s)] to C-9 (δ_c 27.8), C-10 (δ_c 71.4), and C-11 (δ_c 83.0) confirmed the substitution of a hydroxyl group at C-10 and C-11, respectively. The large downfield shifts of C-11 (δ_c 83.0) and the upfield shift of C-15 (δ_c 171.0) in combination with the mass data supported the formation of the lactone ring between C-15 and C-11. The structure of **1** was finally assigned by detailed interpretation of ^1H–^1H COSY and HMBC spectra. The geometry of the double bonds as 2*Z* and 6*Z* were proposed by NOESY correlations of H-2 [δ_H 6.19 (t, *J* = 7.3 Hz)]/H_2-4 [δ_H 2.46 (m)], and H-6 [δ_H 5.14 (t, *J* = 7.2 Hz)]/H_3-14 [δ_H 1.52 (s)] (Fig. 2), respectively. The absolute configuration at C-10 in **1** was determined by the circular dichroism of an in situ formed complex with [$Rh_2(OCOCF_3)_4$], with the inherent contribution subtracted. Upon addition of [$Rh_2(OCOCF_3)_4$] to a solution of **1** in CH_2Cl_2, a metal complex was produced as an auxiliary chromophore. The Rh complex of **1** displayed a negative E band at about 350 nm (Figure 3), correlating with a 10*R* absolute configuration. The alkaline hydrolysis of **1** yielded compound **9,** which further confirmed the structure of **1**. Thus,

compound **1** was assigned as shown, and named as ganoleucin A.

The molecular formula of ganoleucin B (**2**) was established as $C_{21}H_{28}O_4$ by HRTOFMS data at m/z $[M+H]^+$ 345.2060. Its ^1H and ^{13}C NMR spectroscopic data revealed a similar structure to that of **5**. Key differences were that H-2 [δ_H7.01 (t, J = 7.4 Hz)] undergoes large downfield shifts due to de-steric effects.[16] The NOESY correlations of H-1 with H-4, H_2-5 with H_3-14 confirmed the geometry of the double bonds as 2*E* and 6*E*, (Figure 2). The detailed interpretation of 2D NMR spectra established the structure of **2** as shown.

Ganoleucin C (**3**) possessed a molecular formula of $C_{21}H_{24}O_5$ on the basis of HRTOFMS data at m/z $[M+H]^+$ 345.2060. The ^1H and ^{13}C NMR data of **3** resembled those of **4** except for an additional carbonyl carbon at δ_c 196.0 (C-13) and the loss of a methyl group. The above difference indicates that the methyl group at C-13 is replaced by an aldehyde group in compound **3**. The HMBC correlations from H_3-12 [δ_H1.74 (s)] and H-10 [δ_H 6.45 (t, J = 6.7 Hz)] to C-13 (δc196.0) further confirmed the substation of an aldehyde group at C-11(Fig. 2). The relative configuration of 2*Z*, 6*E*, and 10*E* in **3** was elucidated by NOE correlations H-2 [δ_H 6.17 (t, J = 7.3 Hz)]/H-4 [δ_H 2.37 (t, J = 7.2 Hz)], H-6 [δ_H 5.13 (t, J = 6.5 Hz)]/ H-8 [δ_H 2.17 (t, J = 7.2 Hz)], and H-9 [δ_H 2.42 (m)]/H-12 [δ_H 1.74 (s)] (Fig. 2). The comparison of specific rotation data between **7** and **3** confirmed the 2*R* configuration. Thus, the structure of compound **3** was assigned as shown.

*2.2 α-Glucosidase and HMG-CoA reductase inhibitory activity of compounds**1-8.***

α-Glucosidase (EC 3.2.1.20, *α*-D-glucoside glucohydrolase) is exo-acting enzyme that plays essential roles in carbohydrate quality control, processing and metabolism [26]. Postprandial glucose absorption *in vivo* can be attenuated by retarding the cleavage of complex carbohydrates [27]. Therefore, glucosidase inhibitors are applicable to the treatment of numerous disease including diabetes mellitus type-2 [28-34]. 3-hydroxy-3-methylglutaryl co-enzyme A reductase (HMG-CoA reductase) catalyzes the conversion of HMG-CoA to mevalonate, a key precursor of cholesterol biosynthesis [35]. Statins represent the major class of hypolipidemic drugs in the market which act through the inhibition of HMG-CoA reductase [36]. The biological activities of the isolated meroterpenes (**1**-**8**) were assessed against α-glucosidase and HMG-CoA reductase. Compounds **4**, **5**, **7** and **8** inhibited HMG-CoA reductase in a concentration dependent manner with IC_{50} in the range between 12.3 and 56.9 μM.

Compound **1** and **3-8** showed strong inhibitory activity against *α*-Glucosidase from Baker's yeast and rat small intestinal mucosa with the IC_{50} value in the range of 0.3 to 61.2 μM. Among them, ganomycin I (**4**) was found to be the most potent inhibitor against both *α*-glucosidase and HMG-CoA reductase.

We preliminarily analyzed the structure-activity relationship for compounds 1-8 based on above bioassay results. The double bond between C-2 and C-3 and its configuration significantly influences the potency of these inhibitors. Comparing with compound **5**, compound **2** did not exert any inhibitory against α-Glucosidase and HMG-CoA reductase when $\Delta^{2,3}$ bond turned into *E* configuration. The inhibitory activity of **8** (IC_{50} =3.2 μM) was 10-fold more potent than that of compound **6** (IC_{50} =32.1 μM) against α-glucosidase and 2-fold more against HMG-CoA reductase. It can be concluded that the *Z* configuration at $\Delta^{2,3}$ favors inhibitory against both *α*-glucosidase and HMG-CoA reductase.

*2.3 Enzyme kinetic analysis of ganomycin I (**4**) against α-Glucosidase and HMG-CoA reductase.*

The enzyme inhibition property against α-Glucosidase and HMG-CoA reductase of the most potent inhibitor, ganomycin I (**4**), was analyzed by using Lineweaver-Burk and Dixon plots. The initial velocity 'V' of the reaction catalyzed by α-glucosidase and HMG-CoA reductase was determined at different substrate concentrations (S) in the presence and absence of inhibitors (I), as shown in Fig. 4. The double reciprocal plot showed straight lines for ganomycin I (**4**) with p-nitrophenyl-α-D-glucopyranoside (for α-glucosidase assay) and HMG-CoA (for HMG-CoA reductase) as the substrate. Both the slope and vertical axis intercept increase with the enhancement of inhibitor concentration. These results indicated that compound **4** was a noncompetitive inhibitor against both α-glucosidase and HMG-CoA reductase.

2.4 Docking studies on ganomycin I (4) with yeast α-glucosidase

The sequence identity between α-glucosidase (gi number 411229) from baker's yeast and isomaltase (PDB ID: 3A4A) from *Saccharomyces cerevisiae* is 72%. The protein structure validation program PROCHECK predicted that 97.9% residues are in the allowed region, 1.7% residues are in marginal region, only 0.4% are outliers. So the α-glucosidase homology model can be used in the docking.

In Silico docking study of ganomycin I (**4**) with yeast α-glucosidase was then

conducted to confirm the interaction. Ganomycin I (**4**) exhibits a strong binding affinity with the protein by its low binding energy (−10.48 kcal/mol). Fig. 5a. shows the homology model of the yeast α-glucosidase with the ligand docking into the binding site. Fig. 5b. displays the close view of the binding site with the best predicted orientation of ligand ganomycin I (**4**). The molecular docking results showed that the binding pocket involves the amino acid residues Phe157, Phe177, Phe158, Asp214, Thr215, Leu218, His239, Asn241, His245, Gln276, Val277, Ala278, Phe300, Asp349, Gln350, Asp408 and Arg439. There was the H-bond interaction between the hydroxyl group of ganomycin I (4) and Arg439 (the distance: 1.75 Å). And the chain of ganomycin I (4) was inserted into the hydrophobic pocket. This calculation observation is in good agreement with the enzymatic assay where ganomycin I (4) shows a low IC_{50} value (0.3±0.1 μM).

*2.5 Acute toxicity of ganomycin I (**4**).*

Ganomycin I was synthesized according to the reference method.[17] In the acute oral toxicity study, the dosage of ganomycin I (**4**) up to 3 g/kg of body weight did not show any overt symptoms of toxicity (including no apparent differences in physical activity or other behaviors, no significant changes in the nature of stool and urine, no convulsion, sleep or coma) during 24 hours and 14 days' observation. Moreover, no mortality was observed throughout 14 days monitoring.

*2.6 Effects of ganomycin I (**4**) on blood glucose levels and body weight.*

To evaluate the anti-hyperglycemic and hypolipidemic effects for ganomycin I, we used KK-A^y diabetic mice for *in vivo* assay. The clinical drug of rosiglitazone with both antidiabetic and hypolipidemic effects was used as positive control. C57BL/6J mice was treated as normal control group. Ganomycin I (1 mg/kg and 5 mg/kg) was daily administered by gavage method. In KK-A^y mice, sequential monitoring of blood glucose showed that rosiglitazone and ganomycin I (1 and 5 mg/kg groups) decreased the fasted blood glucose and free diet blood glucose after 3-day treatment (Figure 6B and 6C). Glycosylated hemoglobin A1C levels were decreased significantly after a 21-day treatment (Figure 6D). Ganomycin I exhibited equivalent hypoglycemic effect to rosiglitazone. The body weight for each group was measured every three days. The body weight in ganomycin I treated KK-A^y group remained almost unchanged in the course of first two weeks and showed the trend of decrease compared with that of KK-A^y model (Figure 6A and supporting information figure S1). Whereas, the body

weight gained in the rosiglitazone group increased much higher than that of the KK-A^y model.

*2.7 Effects of ganomycin I (**4**) on oral sucrose tolerance test (OSTT).*

In KK-A^y mice, after a 3-week treatment with ganomycin I (**4**), the higher blood glucose level was markedly reversed in OSTT. The Area Under the Curve（AUC） of the ganomycin I (**4**) groups were significantly lower than that in the KK-A^y model group ($P<0.01$) (Figure 7B). These results demonstrated that ganomycin I (**4**) inhibit the action of *α*-glucosidase *in-vivo* efficiently [37,38].

*2.8 Effects of ganomycin I (**4**) on insulin resistance.*

The KK-A^y mice displayed apparent hyperinsulinemia (Figure 8A), and the insulin sensitivity index (ISI) levels decreased with the progress of disease (Figure 8B). Rosiglitazone and all doses of ganomycin I (**4**) significantly decreased the serum insulin levels (Figure 8A) and increased the ISI (Figure 8B). Moreover, In the oral glucose tolerance test (OGTT) and insulin tolerance test (ITT), KK-A^y mice treated by ganomycin I (**4**) showed decrease of blood glucose levels at 30 and 60 min compared with the KK-A^y diabetic mice (Figure 8C and Figure 8E). The AUC of the ganomycin I (**4**) groups in both OGTT and ITT were much lower than that in the control group ($P<0.01$). Overall, ganomycin I, administered at the dose of 5 mg/Kg, presented much stronger efficacy in improving insulin resistance than rosiglitazone.

*2.9 Effects of ganomycin I (**4**) on blood lipids, hepatic glycogen, and AST, ALT.*

As shown in Figure 9, compared with the normal C57BL/6J mice, the KK-A^y diabetic mice showed significant elevation in the levels of blood lipids, including NEFA (Figure 9A), TG (Figure 9B), TC (Figure 9C), LDL-C (Figure 9D), and HDL-C (Figure 9E). After 3 weeks of treatment, the serum NEFA, TG, TC, LDL-C concentrations were significantly lowered in KK-A^y mice treated with ganomycin I (**4**) than that in the KK-A^y diabetic mice ($P<0.01$). In terms of NEFA, TG, and TC, Ganomycin I displayed equivalent hypolipidemic activity to rosiglitazone.

In the KK-A^y mice, via a 4-week treatment with ganomycin I (**4**), the lower liver hepatic glycogen was markedly reversed. The liver hepatic glycogen concentrations of the ganomycin I (**4**) group were significantly higher than that in the control group ($P<0.01$) (Figure 9F). These results demonstrated that ganomycin I (**4**) can promote

the synthesis of hepatic glycogen. The levels of AST and ALT in the serum of the C57BL/6J and KK-A^y mice were presented in Figure 9G and 9H. KK-A^y diabetic mice exhibited much higher serum ALT and AST than C57BL/6J mice. Following the 3-week treatment with ganomycin I (**4**), the serum AST level was significantly decreased. Rosiglitazone did not show any activity on the level of AST and the synthesis of hepatic glycogen.

2.10 Histopathological examination

Histological analysis of liver. Coincident with increased hepatic TG content ($P<0.05$), the untreated KK-A^y mice showed hypertrophy of hepatocytes and hepatic steatosis (Figure 10A). Unlike rosiglitazone, which had no obvious impact on hepatic TG and TC contents in KK-A^y mice, ganomycin I (5 mg/kg) ameliorated the hepatocyte hypertrophy and significantly lowered the lipid droplet accumulation.

Histological analysis of adipose tissue. In KK-A^y mice, both rosiglitazone and ganomycin I (**5** mg/kg) decreased the size of the adipocytes in WAT, indicating the increase in number of adipose cells.

3. Conclusion

In conclusion, three new meroterpenoids, Ganoleucin A-C (**1**-**3**), together with 5 known meroterpenoids (**4**-**8**), were isolated and identified from the fruiting bodies of *Ganoderma leucocontextum*. The inhibitory effects of **1**-**8** on HMG-CoA reductase and α-glucosidase were tested *in vitro*. Ganomycin I (**4**), **5**, and **8** showed stronger inhibitory activity against HMG-CoA reductase than the positive control atorvastatin. Compounds **1**, and **3**-**8** presented potent noncompetitive inhibitory activity against α-glucosidase. Preliminary structure-activity relationship (SAR) analysis indicated that the existence and geometry of the double bond between C-2 and C-3 play an important role in the inhibitory activity against both HMG-CoA reductase and α-glucosidase.

Ganomycin I (**4**), the most potent inhibitor against both *α*-glucosidase and HMG-CoA reductase, was further evaluated for its *in vivo* bioactivity. Ganomycin I (**4**) exhibited potent and efficacious hypoglycemic, hypolipidemic, and insulin-sensitizing effects in KK-A^y mice. Based on the results obtained in the current study, we suppose that ganomycin I (**4**) could be a promising anti-diabetic and anti-lipidemic candidate for new drug developments. The action mechanism, *in vivo* efficacy, and long term

toxicity of ganomycin I (**4**) deserve further investigation.

4. Materials and methods

4.1 General apparatus and chemicals.

Solvent used for extraction and chromatographic separation was analytical grade. TLC was carried out on Silica gel HSGF254 and compounds were visualized by spraying with 10% H_2SO_4 and heating. Silica gel (Qingdao Haiyang Chemical Co., Ltd., People's Republic of China) and Sephadex LH-20 (Amersham Biosciences) were used for column chromatography. HPLC separation was performed on an Agilent 1200 HPLC system using an ODS column (C18, 250 × 9.4 mm, YMC Pak, 5 □m; detector: UV) with a flow rate of 2.0 mL/min. UV and IR spectral data were acquired using a ThermoGenesys-10S UV-Vis and Nicolet IS5 FT-IR spectrophotometer, respectively. Optical rotations were measured on an Anton Paar MCP 200 Automatic Polarimeter. NMR spectral data was obtained with Bruker Avance-500 spectrometer ($CDCl_3$, δ_H 7.26/ δ_C 77.16). The HSQC and HMBC experiments were optimized for 145.0 and 8.0 Hz, respectively. HRTOFMS data was measured using an Agilent Accurate-Mass-Q-TOF LC/MS 6520 instrument.

4.2 Fungal Material.

The fungi *G. leucocontextum* were collected in Nyingchi, Tibet, China in 2015, and identified by Xin-cun Wang (Institute of Microbiology, Chinese Academy of Sciences) comparing its morphological characteristic with those published for *G. leucocontexum* [22].

4.3 Extraction and Isolation.

The air-dried and powdered fruiting bodies of *G. leucocontexum* (5 kg) were extracted three times with ethyl alcohol (3 × 20 L), and organic solvent was evaporated to dryness under vacuum to afford the crude extract (233 g). The ethanol extract was partitioned between ethyl acetate and water. The EtOAc extract (90.5 g) was subjected to silica gel column chromatography (CC) using hexane-ethyl acetate in a gradient elution (v/v, 100:0, 100:2, 100:5, 100:8, 100:10, 100:15, 100:20, 100:40, 100:50), followed by dichloromethane-methanol elution (v/v, 100:1, 100:2, 100:3, 100:5, 100:10, 100:15, 100:20, 0:100) to give 9 fractions (GL-1−GL-9). Fraction 6 (10.45 g) eluted with dichloromethane-methanol (*v/v*, 50:1) was further separated on Sephadex LH-20 CC eluted with 50% methanol in water to give 7 subfractions (GL-

6-1−GL-6-7). Compounds **1** (3.2 mg, t_R 24.1 min) and **3** (12.3 mg, t_R26.2min) were purified from subfraction GL-6-2 (40.2 mg) by RP-HPLC using 52% acetonitrile in water. Compounds **2** (16.2 mg, t_R 36.2 min), **4** (30.2 mg, t_R 38.9 min), and **5** (10.1 mg, t_R 40.1 min) were isolated from GL-6-3 (120.2mg) by RP-HPLC using 48% acetonitrile in water. Subfraction GL-6-5 (202.3 mg) was separated by RP-HPLC using 45 % acetonitrile in water to afford compound **6** (23.1 mg, t_R 22.1 min). Compounds **7** (22.3 mg, t_R 22.5 min), **8** (8.2 mg, t_R 24.2 min) were purified from fraction GL-6-6 (90.2 mg) by RP-HPLC using 65% methanol in water. The physical properties, spectroscopic data of the new compounds are as follows.

*4.3.1Ganoleucin A (**1**)*

Colorless powder, $[\alpha]^{25}_D$ +25.10 (*c* 0.1, MeOH); UV (MeOH) λ_{max} (log ε) 211 (4.10), 320 (2.05) nm; IR (neat) ν_{max} 3310, 2845, 2810, 1685, 1435, 1323, 122245, 723 cm^{-1}; for ^1H and ^{13}C NMR data see Tables 1; positive HRTOFMS *m/z* [M+ H] $^+$ 361.2011 (calcd. for $C_{21}H_{28}O_5$, 361.2011).

*4.3.2 Ganoleucin B (**2**)*

Colorless powder, $[\alpha]^{25}_D$ +2.00 (*c* 0.1, MeOH); UV (MeOH) λ_{max} (log ε) 210 (3.54), 315 (2.00) nm; IR (neat) ν_{max} 3310, 1723, 1725, 1623, 1470, 1325, 1222, 725, 623 cm^{-1}; for ^1H and ^{13}C NMR data see Tables 1; positive HRTOFMS *m/z* [M+ H] $^+$ 345.2060 (calcd. for $C_{21}H_{28}O_4$, 345.2064).

*4.3.3 Ganoleucin C (**3**)*

Yellow powder, $[\alpha]^{25}_D$ +36.20 (*c* 0.1, MeOH); UV (MeOH) λ_{max} (log ε) 220 (2.10), 320 (2.45) nm; IR (neat) ν_{max} 3335, 2986, 2928, 2836, 1725, 1711, 1645, 1612, 1488, 1345, 1324, 1235, 736, 625 cm^{-1}; for ^1H and ^{13}C NMR data see Tables 1; positive HRTOFMS *m/z* [M+H] $^+$357.1697 (calcd. for $C_{21}H_{24}O_5$, 357.1695).

*4.4 Absolute configuration of the C-10 in **1*** [39].

A sample of **1** (1 mg) was dissolved in a dry solution of $CHCl_3$ (0.5 mL). The starting CD spectrum was recorded. Then, the $CHCl_3$ solution of **1** was mixed with $[Rh_2(OCOCF_3)_4]$ complex (1.1 mg), and reaction's time evolution was monitored until stationary (5 min after mixing). The inherent CD was subtracted. The observed sign of the E band at 350 nm in the induced CD spectrum was correlated to the absolute configuration of the C-10 moiety.

*4.5 Alkaline Hydrolysis of Compound **1**.*

According to a published procedure [40], compound **1** (3.0 mg) dissolved in 2% sodium methylate-methanol (4 mL) was stirred at room temperature for 1 h. The reaction mixture was neutralized with 10% acetic acid. After removal of the solvent from the filtrate under reduced pressure, the residue was dissolved in water (10 mL) and extracted with ethyl acetate (10 mL). The organic solvents were evaporated and purified by preparative TLC on silica gel (dichloromethane: methanol, 20:1) to give compound **9** (1.8 mg).

*4.6 Synthesis of ganomycin I (**4**).*

The chemical synthesis of ganomycin I (**4**) is operated as the original synthesis donor of *Yajima et al.* [17], which proved to be effective in this compound (supporting information scheme 1).

4.7 Inhibition Assay against α-Glucosidase from Baker's yeast

As described in our earlier work [41], the bioassay was conducted using a 96-well plate, and the absorbance was determined at 405 nm using a Spectra Max 190 microplate reader (Molecular Devices Inc.). The control was prepared by adding a phosphate buffer instead of tested compounds. The blank was prepared by adding phosphate buffer instead of the α-glucosidase. The inhibition rates (%) = [(OD $_{control}$ - OD $_{control\ blank}$) - (OD $_{test}$ - OD $_{test\ blank}$)]/ (OD $_{control}$ - OD $_{control\ blank}$) × 100%. Acarbose was utilized as the positive control with an IC_{50} of 273.1 μM.

4.8 Inhibition Assay against α-Glucosidase, Sucrase, and Maltase from Rat's Small Intestinal Mucosa

A slightly modified method of the rat intestinal mucosa assay developed by Kwon et al. was used [42,43]. Each compound dissolved in DMSO (10 μL) was mixed with 20 μL of substrate (maltose, sucrose, p-nitrophenyl-α-D-glucopyranoside, respectively), 10 μL of enzyme solution, and 60 μL of 0.1 M phosphate buffer (pH 6.9). After pre-incubation for 40 minutes, a commercial kit (GOD assay, Jiancheng Biological Engineering Institute, Najing, China) was used to test the production of glucose. The absorbance was read at 550 nm under a Spectra Max 190 microplate reader (Molecular Devices Inc.). The blank was prepared by adding potassium phosphate buffer instead of enzyme. The control was prepared by adding potassium

phosphate buffer instead of tested compounds. The inhibition rates (%) = [(OD $_{control}$ - OD $_{control\ blank}$) - (OD $_{test}$ - OD $_{test\ blank}$)] / (OD $_{control}$ - OD $_{control\ blank}$) × 100%.

4.9 Inhibition Assay against HMG-CoA Reductase.

As described in our earlier work [13], The assay was conducted in a 96-well plate, and the absorbance was determined at 340 nm using a Spectra Max 190 microplate reader (Molecular Devices Inc.). The blank was prepared by adding potassium phosphate buffer instead of HMG-CoA reductase. The control was prepared by adding potassium phosphate buffer instead of tested compounds. The inhibition rates (%) = [(OD $_{test}$ - OD $_{test\ blank}$) - (OD $_{control\ blank}$ - OD $_{control}$)] / (OD $_{control\ blank}$ - OD $_{control}$) × 100%.

4.10 Enzyme inhibition kinetic

The type of inhibition of α-glucosidase and HMG-CoA Reductase by compound 4 (in the concentrations of 0.3 to 1 μM for α-glucosidase and 5 to 20 μM for HMG-CoA Reductase) was established by using the Michaelis-Menton equation and Lineweaver-Burk plots. *p*-NPG and HMG-CoA, in the concentrations of 2 μM, 4 μM, 6 μM, and 8 μM, were used as substrates.

4.11. Molecular modeling and docking studies

The sequence of *Saccharomyces cerevisiae* (baker's yeast) α-glucosidase (gi number 411229) was taken from the protein sequence data bank (http:// www.ncbi.nlm.nih.gov/protein/), and the crystal structure of isomaltase from *Saccharomyces cerevisiae* (pdb code: 3A4A) [44] was selected as template by blasting. The α-glucosidase homology model was generated using MODELLER9v3 [45]. The final α-glucosidase model was validated by the Ramachandran plot using the PROCHECK program [46].

Molecular docking simulation was performed using GADock from ArgusLab [47]. The dimensions for the cubic boundary box centered on the centroid of Asp349 were set to 25 Å × 25 Å × 25 Å. Docking behavior was predicted using genetic algorithm method: a population size of 100 with 3,000 generations, a gene mutation rate of 0.02, and a crossover of 0.8. The final ligand-protein complex was visualized using PyMOL 0.99 [48].

4.12 Animal and treatment

All procedures were performed in accordance with the standards of the Department of Health and Human Services and under protocols approved by the Novartis Animal Care and Use Committee. Care and husbandry followed standard guidelines.

4.12.1 KK-A^y mouse study.

Normal female C57BL/6*J* mice (8 weeks old) and insulin-resistant male KK-A^y mice (8 weeks old) were purchased from the Experimental Animal Center, Chinese Academy of Medical Sciences. Both C56BL/6*J* and KK-A^y mice were provided with a high-fat diet and water *ad libitum*. At the beginning of the study, KK-A^y mice were weighed, bled via the tail vein in the fasted state (4 h) and sorted into four groups (n = 8 each) based on their blood glucose levels and initial body weight: Rosiglitazone (10 $mg \cdot kg^{-1} \cdot day^{-1}$), ganomycin I (**4**) (1, 5 $mg \cdot kg^{-1} \cdot day^{-1}$ respectively), and KK-A^y model. C57BL/6*J* mice were weighed and sorted into C57BL/6*J* control group. All five groups were administered by gavage once a day for 21 days. Individual body weight and cage food consumption were measured every 3 days. At the end of the experimental period, blood samples were collected for immediate assessment of serum biochemical parameters.

4.12.2 Metabolic studies

Serum glucose, total cholesterol (TCHO), triglycerides (TG), non-esterified fatty acids (NEFA), high density lipoprotein cholesterol(HDL-C), low density lipoprotein cholesterol(LDL-C), and insulin levels were measured as Chen *et al.* described [49]. The insulin sensitivity index (ISI) was calculated from the values of FBG and fasting blood insulin (FBI). ISI=1/(FBG*FBI)1000, where FBG is expressed as $mg \cdot dL^{-1}$ and FBI as $mU \cdot L^{-1}$.

4.12.3 Oral sucrose tolerance test (OSTT)

OSTT was performed by giving a sucrose bolus (4 $g \cdot kg^{-1}$) by gavage after overnight fasting. Glycaemia was measured through the tail tip before and after glucose load at the times indicated. The area under the curves (AUC)generated from the data collected during the OSTT was calculated.

4.12.4 Insulin tolerance test (ITT)

ITT was performed by giving an insulin injection (0.6 $U \cdot kg^{-1}$) by intraperitoneal injection after a 4 hours fasting. Glycaemia was measured through the tail tip before and after insulin injection at the times indicated. The area under the curves (AUC) generated from the data collected during the ITT was calculated.

4.12.5 Oral glucose tolerance test (OGTT)

OGTT was performed by giving a glucose bolus (2 $g \cdot kg^{-1}$) by gavage after overnight fasting. Glycaemia was measured through the tail tip before and after glucose load at the times indicated. The area under the curves (AUC) generated from the data collected during the OGTT was calculated.

4.12.6 Histopathological examination and electron microscopy

Samples of liver, abdominal white adipose tissue (WAT) were resected and fixed with 10% formaldehyde phosphate buffered saline (pH 7.4), then embedded in paraffin, sectioned, stained with haematoxylin/eosin and analyzed by either microscopy or morphometry.

4.13 Statistical analysis

All results are expressed as mean ±SEM. For multiple comparisons, the statistical analysis was performed by using one-way or two-way ANOVA followed by the Tukey's multiple comparison tests with Graph Pad 6.0. $P < 0.05$ was considered to be statistically significant.

Acknowledgments

Financial supports of the National Nature Science Foundation (21472233), the Ministry of Science and Technology of China (2014CB138304), the Youth Innovation Promotion Association of Chinese Academy of Sciences (2014074) and Open Fund of Hubei Key Laboratory of Natural Products Research and Development (China Three Gorges University) (2016NP09) are acknowledged. Dr. Jinwei Ren and Dr. Wenzhao Wang (State Key Laboratory of Mycology, Institute of Microbiology, Chinese Academy of Sciences) are appreciated for their help in measuring the NMR and MS data.

Supporting information

NMR spectra data of compounds **1**-**9**; synthesis of ganomycin I (**4**); ^{1}H and ^{13}C

NMR data of **4-8**. This material is available free of charge via the Internet at http://dx.doi.org.

References

[1] Grundy, S.M. What is the contribution of obesity to the metabolic syndrome? *Endocrinol. Metab. Clin. North. Am.* 33 (2004) 267–82.

[2] Haffner, S.; Taegtmeyer, H. Epidemic obesity and the metabolic syndrome. *Circulation.*108 (2003) 1541–5.

[3] Lebovitz, H.E. The relationship of obesity to the metabolic syndrome. *Int. J. Clin. Pract. Suppl.*134 (2003) 18–27.

[4] Bjorntorp, P. Abdominal obesity and the metabolic syndrome. *Ann. Med.* 24 (1992) 465–468.

[5] Turkoglu, C.; Duman, B.S.; Gunay, D.; Cagatay, P.; Ozcan, R.; Buyukdevrim, A.S. Effect of abdominal obesity on insulin resistance and the components of the metabolic syndrome: evidence supporting obesity as the central feature. *Obes. Surg.* 13 (2003) 699–705.

[6] Sanodiya, B.S.; Thakur, G.S.; Baghel, R.K.; Prasad, G.B.; Bisen, P. S. *Ganoderma lucidum*: a potent pharmacological macrofungus. *Curr. Pharm.Biotechnol.*10 (2009) 717–742.

[7] Agius, L. New hepatic targets for glycaemic control in diabetes. Best practice and research. *Clin. Endocrinol. Metab.* 21 (2007) 587–605.

[8] McCormack, J.G.; Westergaard, N.; Kristiansen, M.; Brand, C.L.; Lau, J.; Pharmacological approaches to inhibit endogenous glucose production as a means of anti-diabetic therapy. *Curr. Pharm. Des.* 7 (2001) 1451–1474.

[9] Fatmawati, S.; Kurashiki, K.; Takeno, S.; Kim, Y.U.; Shimizu, K.; Sato, M.; Imaizumi, K.; Takahashi, K.; Kamiya, S.; Kaneko, S.; Kondo, R. The inhibitory effect on aldose reductase by an extract of *Ganoderma lucidum. Phytother. Res. PTR* 23 (2009) 28–32.

[10] Pan, D.; Wang, L.; Hu, B.; Zhou, P. Structural characterization and bioactivity evaluation of an acidic proteoglycan extract from *Ganoderma lucidum* fruiting bodies for PTP1B inhibition and anti-diabetes. *Biopolymers* 101 (2014), 613–623.

[11] Shiao, M.S.; Lee, K.R.; Lin, L.J.; Wang C.T. Natural products and biological activities of the Chinese medicinal fungus *Ganoderma lucidum, ACS Symp. Ser.* 547 (1994) 342–354.

[12] Xia, Q.; Zhang, H.; Sun, X.; Zhao, H.; Wu, L.; Zhu, D.; Yang, G.; Shao, Y.; Zhang, X.; Mao, X.; Zhang, L.; She, G. A comprehensive review of the structure elucidation and biological activity of triterpenoids from *Ganoderma* spp. *Molecules* 19 (2014) 17478–17535.

[13] Wang K.; Bao, L.; Xiong, W. P.; Ma, K.; Han, J.J.; Wang, W.Z.; Yin, W.B.; Liu, H.W. Lanostane triterpenes from the Tibetan medicinal mushroom *Ganoderma leucocontextum* and their inhibitory effects on HMG-CoA reductase and alpha-glucosidase, *J. Nat. Prod.* 78 (2015) 1977–1989.

[14] Dou, M.; Di, L.; Zhou, L.L.; Yan, Y.M.; Wang, X.L.; Zhou, F.J.; Yang, Z.L.; Li, R.T.; Hou, F.F.; Cheng, Y.X. Cochlearols A and B, Polycyclic Meroterpenoids from the Fungus *Ganoderma cochlear* That Have Renoprotective Activities. *Org. Lett.*16 (2014), 6064-6067.

[15] Luo, Q.; Di, L.; Dai, W.F.; Lu, Q.; Yan, Y.M.; Yang, Z.L.; Li, R.T.; Cheng, Y.X. Applanatumin A, a New Dimeric Meroterpenoid from *Ganoderma applanatum* That Displays Potent Antifibrotic Activity. *Org. Lett.*17 (2015) 1110-1113.

[16] Huang, S.Z.; Cheng, B.H.; Ma, Y.Q.; Wang, Q.; Kong, F.D.; Dai, F.H.; Qiu, S.Q.; Zheng, P.Y.; Liu, Z.Q.; Zhao, Y.X. Anti-allergic prenylated hydroquinones and alkaloids from the fruiting body of *Ganoderma calidophilum*. *RSC Adv.* 6 (2016) 21139-21147.

[17] Yajima, A.; Urao, S.; Katsuta, R.; Nukada, T. Concise Syntheses and Biological Activities of Ganomycin I and Fornicin A. *Eur. J. Org. Chem.* 4 (2014) 731-738

[18] Luo, Q.; Wang, X.L.; Di, L.; Yan, Y.M.; Lu, Q.; Yang, X.H.; Hu, D.B.; Cheng, Y.X. Isolation and identification of renoprotective substances from the mushroom *Ganoderma lucidum*. *Tetrahedron* 71 (2015) 840-845.

[19] Yan, Y.M.; Ai, J.; Zhou, L.L.; Chung, C.L.; Li, R.; Nie, J.; Fang, P.; Wang, X.L.; Luo, J.; Hu, Q.; Hou, F.F.; Cheng, Y.X. Lingzhiols, Unprecedented Rotary Door-Shaped Meroterpenoids as Potent and Selective Inhibitors of p-Smad3 from *Ganoderma lucidum*. *Org. Lett.* 15 (2013) 5488-5491.

[20] Peng, X.R.; Liu, J.Q.; Wan, L.S.; Li, X.N.; Yan, Y.X.; Qiu, M.H.Four New Polycyclic Meroterpenoids from *Ganoderma cochlear*.*Org. Lett.*16 (2014) 6064-6067.

[21] Zhou, F.J.; Nian, Y.; Yan, Y.M.; Gong, Y.; Luo, Q.; Zhang, Y.; Hou, B.; Zuo, Z.L.; Wang, S.M.; Jiang, H.H.; Yang, J.; Cheng, Y.X. Two New Classes of T Type Calcium Channel Inhibitors with New Chemical Scaffolds from *Ganoderma cochlea*r. *Org.*

Lett. 17 (2015) 3082-3085.

[22] Li, T.H.; Hu, H.P.; Deng, W.Q.; Wu, S.H.; Wang, D.M.; Tsering, T. *Ganoderma leucocontextum,* a new member of the *G. lucidum* complex from southwestern China. *Mycoscience* 56 (2014) 81-85.

[23] Mothana, R.A.A.; Jansen, R.; Julich, W.D.; Lindequist, U. Ganomycins A and B, new antimicrobial farnesyl hydroquinones from the basidiomycete *Ganoderma pfeifferi. J. Nat. Prod.* 63 (2000) 416-418.

[24] Niu, X.M.; Li, S.H.; Sun, H.D.; Che, C.T. Prenylated phenolics from *Ganoderma fornicatum. J. Nat. Prod.*69 (2006) 1354-1365.

[25] Huang, S.Z.; Cheng, B.H.; Ma, Q.Y.; Wang, Q.; Kong, F.D.; Dai, H.F.; Qiu, S.Q.; Zheng, P.Y.; Zhao, Y.X. Anti-allergic prenylated hydroquinones and alkaloids from the fruiting body of *Ganoderma calidophilum.*

[26] Bojarova, P; Kren, V. Glycosidases: a key to tailored carbohydrates. *Trends Biotechnol*. 27 (2009) 199-209.

[27] Maki, K.C.; Carson, M.L.; Miller, M.P.; Turowski, M.; Bell, M.; Wilder, D.M.; Reeves, M.S. High-viscosity hydroxypropylmethylcellulose blunts postprandial glucose and insulin responses, *Diabetes Care* 30 (2007) 1039-1043.

[28] Fernandes, B.; Sagman, U.; Auger, M.; Demetrio, M.; Dennis, J.W β1-6 Branchedoligo saccharides as a marker of tumor progression in human breast and colonneoplasia. *Cancer Res.* 51 (1991) 718-723.

[29] Seiichiro, O; Ayako, M.; Takashi, O.; Hideya, Y.; Hironobu, H. Synthesis and biological evaluation of α-L-fucosidase inhibitors: 5α-carba-α-L-fucopyranosyl-amine and related compounds. *Eur. J. Org. Chem.* 5 (2001) 967-974.

[30] Taha, M.; Ismail, N.H.; Imran, S.; Wadood, A.; Ali, M.; Rahim, F.; Khan, A.A.; Riaz, M. Novel thiosemicarbazide-oxadiazole hybrids as unprecedented inhibitors of yeast alpha-glucosidase and in silico binding analysis. *RSC Adv.* 6(2016) 33733-33742.

[31] Khan, K.M.; Qurban, S.; Salar, U.; Taha, M.; Hussain, S.; Perveen, S.; Hameed, A.; Ismail, N.H.; Riaz, M.; Wadood, A. Synthesis, in vitro alpha-glucosidase inhibitory activity and molecular dockingstudies of new thiazole derivativ es. *Bioorg. Chem.* 68(2016) 245-258.

[32] Zawawi, N.K.N.A.; Taha, M.; Ahmat, N.; Wadood, A.; Ismail, N.H.; Rahim, F.; Azam, S.S.; Abdullah, H. Benzimidazole derivatives as new alpha-glucosidase inhibitors and in silico studies. *Bioorg. Chem.* 64(2016) 29-36.

[33] Salar, U.; Taha, M.; Khan, K.M.; Ismail, N.H.; Imran, S.; Perveen, S.; Gul, S.; Wadood, A. Syntheses of new 3-thiazolyl coumarin derivatives, in vitro alpha-glucosidase inhibitory activity, and molecular modeling studies. *Eur. J. Med. Chem.* 122(2016) 196-204.

[34] Imran, S.; Taha, M.; Ismail, N.H.; Kashif, S.M.; Rahim, F.; Jamil, W.; Wahab, H.; Khan, K.M. Synthesis, in vitro docking studies of new flavone ethers as alpha-glucosidease inhibitors. *Chem. Biol. Drug. Des.* 87 (2016) 361-373.

[35] Friesen, J.A.; Rodwell, V.W. The 3-hydroxy-3-methylglutaryl coenzyme-A (HMG-CoA) reductases. *Genome Biol.* 5 (2004) 248

[36] Istvan, E.S.; Deisenhofer, J. Structural mechanism for statin inhibition of HMG-CoA reductase. *Science* 292(2001) 1160-1164.

[37] Enc, F.Y.; Imeryuz, N.; Akin, L.; Turoglu, T.; Dede, F.; Haklar, G.; Tekesin, N.; Bekiroglu, N.; Yegen, B.C.; Rehfeld, J.F. Holst, J.J.; Ulusoy, N.B. Inhibition of gastric emptying by acarbose is correlated with GLP-1 response and accompanied by CCK release. *Am. J. Physiol-Gastr. L.* 281 (2001) G752-G763.

[38] Chen, H.H.; Chen, D.Y.; Chao, Y.H.; Chen, Y.M.; Wu, C.L.; Lai, K.L.; Lin, C.H.; Lin, C.C. Acarbose Decreases the Rheumatoid Arthritis Risk of Diabetic Patients and Attenuates the Incidence and Severity of Collagen-induced Arthritis in Mice. *Sci. Rep.* 5 (2015) 18288.

[39] J. Liu, Y.B. Liu, Y.K. Si, S.S. Yu, J. Qu, S. Xu, Y.C. Hu, S.G. Ma, New vernocuminosides from the stem barks of *Vernonia cumingiana* Benth *Steroids* 74(2009) 51-61.

[40] Ma, K.; Han, J.J.; Jin, T.; Yang, X.L.; Zhao, F.; Li, S.F.; Song, F.H.; Liu, M.M.; Liu, H.W. New benzoate derivatives and hirsutane type sesquiterpenoids with antimicrobial activity and cytotoxicity from the solid-state fermented rice by the medicinal mushroom *Stereum hirsutum. Food Chem.* 143 (2014**)** 239-245.

[41] Ma, K.; Han, J.J.; Bao, L.; Wei, T.Z.; Liu, H.W. Two Sarcoviolins with Antioxidative and α-Glucosidase Inhibitory Activity from the Edible Mushroom *Sarcodon leucopus* Collected in Tibet. *J. Nat. Prod.* 77 (2014) 942-947.

[42] Kwon, Y.I.; Vattem, D.A.; Shetty, K.Evaluation of clonal herbs of Lamiaceae species for management of diabetes and hypertension. *Asia Pac. J. Clin. Nutr.* 15 (2006) 107-118.

[43] Thao, N.P.; Luyen, B.T.T.; Tai, B.H.; Yang, S.Y.; Jo, S.H.; Cuong, N.X.; Nam, Y.I.; Kwon, Y.I.; Minh, C.V.; Kim, Y.H. Rat intestinal sucrase inhibition of

constituents from the roots of *Rosa rugose* Thunb. *Bioorg. Med. Chem. Lett.* 24 (2014) 1192-1196.

[44] Yamamoto, K.; Miyake, H.; Kusunoki, M.; Osaki, S. Crystal structures of isomaltase from Saccharomyces cerevisiae and in complex with its competitive inhibitor maltose. *Febs J.* 277 (2010): 4205-4214.

[45] Sali A.; Blundell T.L. Comparative protein modelling by satisfaction of spatial restraints. *J. Mol. Biol.* 234(1993):779–815.

[46] Laskowski R.A.; MacArthur M.W.; Moss D.S.; Thomton J.M. PROCHECK: a program to check the stereochemical quality of protein structures. *J Appl Crystallogr* 26 (1993):283–291

[47] Thompson M.A. (2004) Argus Lab 4.0.1. Planaria Software, LLC, Seattle.

[48] DeLano W.L. (2004) The PyMOL molecular graphics system. DeLano Scientific, San Carlos

[49] Chen, W.; Zhou, X.B.; Liu, H.Y.; Xu, C.; Wang, L.L.; Li, S. P633H, a novel dual agonist at peroxisome proliferator-activated receptors α and γ, with different anti-diabetic effects in *db/db* and KK-A^y mice. *Brit. J. Pharmacol.* 157 (2009) 724-735.

Legends

Figure 1. Structures of compounds **1-9.**

Figure 2. Key ^{1}H–^{1}H COSY, HMBC, and NOSEY correlations of **1-3**

Figure 3. Experimental CD spectrum of the Rh complex of **1** with the inherent CD spectrum subtracted.

Figure 4. Line-weaver -Burk plot (1/V vs 1/[S]) for ganomycin I (**4**). (A) against α-glucosidase using pNPG as substrate. (B) against HMG-CoA reductase using HMG-CoA as substrate.

Figure 5. (a) Homology model of the yeast a-glucosidase with the ligand (green color) into the binding site. surrounding the binding site, the amino acid was labeled in green (b).

Figure 6. Effects of ganomycin I (**4**) on body weight and blood glucose levels. (A) Body weight in KK-A^y mice, (B) Sequential monitoring of blood glucose in KK-A^y mice after 4h fasting, (C) Free diet blood glucose in KK-A^y mice, (D) HbA1c in KK-A^y mice. Values are means ±SEM (n = 8 for KK-A^y mice); **P*<0.05, ***P*<0.01, ****P*<0.001 versus KK-A^ymodel group. Con, ⊷, C57BL/6J mice control; KK-M, ⊷,KK-A^y model; Ros-10, ⊷, rosiglitazone 10 mg/kg; GI-h, ⊷ ganomycin I (**4**) 5 mg/kg; GI-l, ⊷ GI-l 1 mg/kg.

Figure 7. Effects of ganomycin I (**4**) on oral sucrose tolerance test (OSTT). (A) OSTT and (B) AUC of the OSTT on the 20th day of treatment in KK-A^y mice. Values are means ±SEM. (n = 8 for KK-A^y mice); **P*<0.05, ***P*<0.01, ****P*<0.001 versus KK-A^y model group. Con, ⊷, C57BL/6J mice control; KK-M, ⊷,KK-A^y model; Ros-10, ⊷, rosiglitazone 10 mg/kg; GI-h, ⊷ ganomycin I (**4**) 5 mg/kg; GI-l, ⊷ GI-l 1 mg/kg.

Figure. 8 Effects of ganomycin I (**4**) on insulin resistance. (A) Serum insulin in KK-A^y mice, (B) ISI in KK-A^y mice, (C) OGTT and (D) AUC of OGTT on the 21th day of treatment in KK-A^y mice. (E) ITT and (F) AUC of the ITT on the 19th day of treatment in KK-A^y mice. Values are means ±SEM (n = 8 for KK-A^y mice); **P*<0.05, ***P*<0.01, ****P*<0.001versus KK-A^y model group. Con, ⊷, C57BL/6J mice control; KK-M, ⊷,KK-A^y model; Ros-10, ⊷, rosiglitazone 10 mg/kg; GI-h,

ganomycin I (**4**) 5 mg/kg; GI-l, GI-l 1 mg/kg.

Figure 9. Effects of ganomycin I (**4**) on AST, ALT, blood lipids. (A) Serum NEFA in KK-A^y mice, (B) Serum TG in KK-A^y mice (C) Serum TC in KK-A^y mice and (D) Serum LDL-C in KK-A^y mice, (E) Serum HDL-C in KK-A^y mice, (F) liver hepatic glycogen in KK-A^y mice (G) Serum AST in KK-A^y mice, (H)Serum ALT in KK-A^y mice. Values are mean ±SEM (n = 7-8 for KK-A^y mice); **P*<0.05, ***P*<0.01, ****P*<0.001 versus KK-A^y model group. Con, C57BL/6J mice control; KK-M, KK-A^y model; Ros-10, rosiglitazone 10 mg/kg; GI-h, ganomycin I (**4**) 5 mg/kg; GI-l, GI-l 1 mg/kg.

Figure 10. Photomicrographs of liver, WAT sections of the KK-A^y mice treated with ganomycin I (**4**). (A) Liver. Hypertrophy of hepatocytes and hepatic steatosis are evident. (B) WAT. (HE: 20×). Con, C57BL/6J mice control; KK-M, KK-A^y model; Ros-10, rosiglitazone 10 mg/kg; GI-h, ganomycin I (**4**) 5 mg/kg;

Table 1. ^{1}H and ^{13}C NMR data of **1-3** (in $CDCl_3$)

Table 2. HMG-CoA reductase and α-Glucosidase inhibitory activity of **1-8**

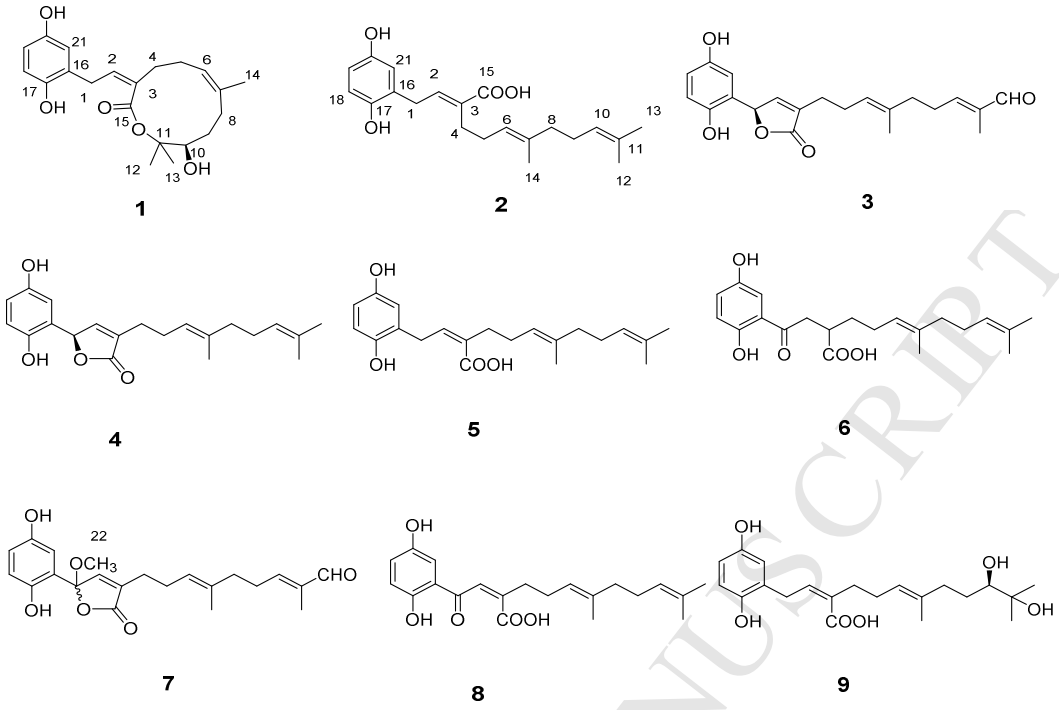

Figure 1. Structures of compounds **1-9.**

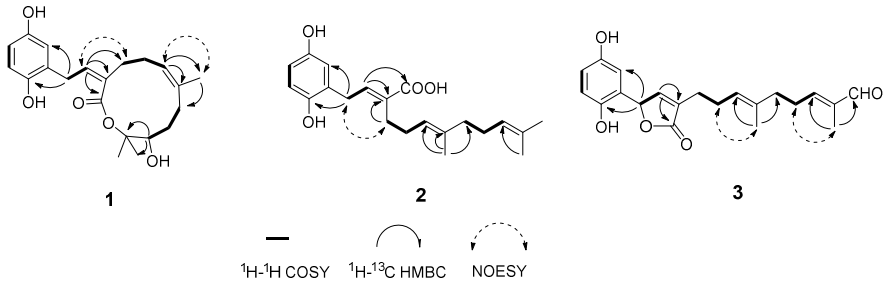

Figure 2. Key ^{1}H–^{1}H COSY, HMBC, and NOSEY correlations of **1-3**

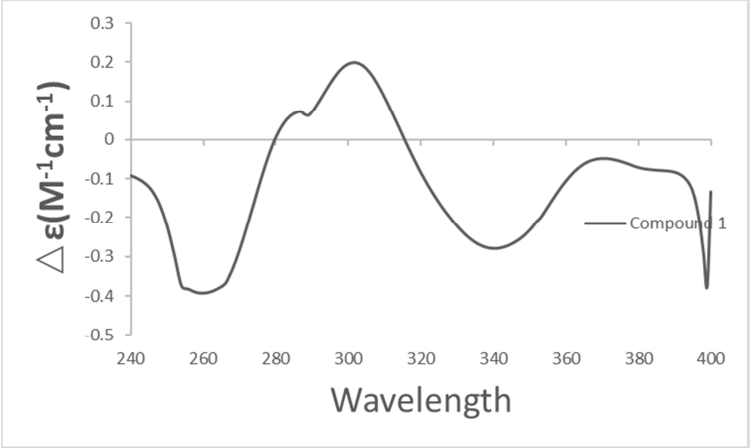

Figure 3. Experimental CD spectrum of the Rh complex of **1** with the inherent CD spectrum subtracted.

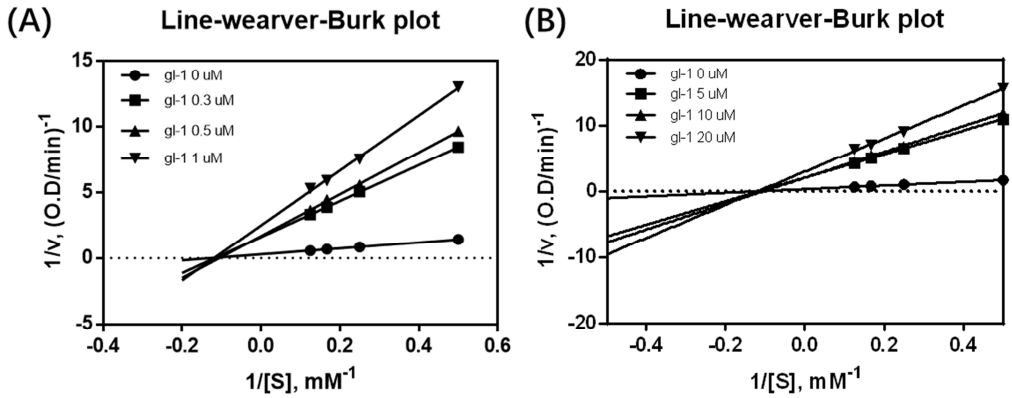

Figure 4. Line-weaver -Burk plot (1/V vs 1/[S]) for ganomycin I (**4**). (A) against α-glucosidase using pNPG as substrate. (B) against HMG-CoA reductase using HMG-CoA as substrate.

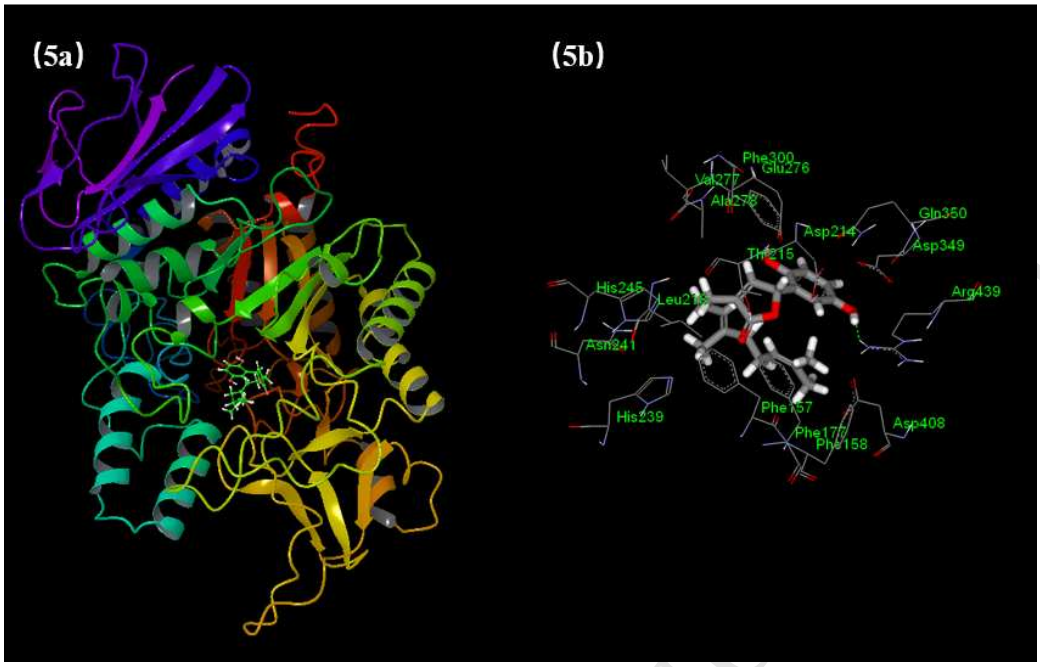

Figure 5. (a) Homology model of the yeast a-glucosidase with the ligand (green color) into the binding site. surrounding the binding site, the amino acid was labeled in green (b).

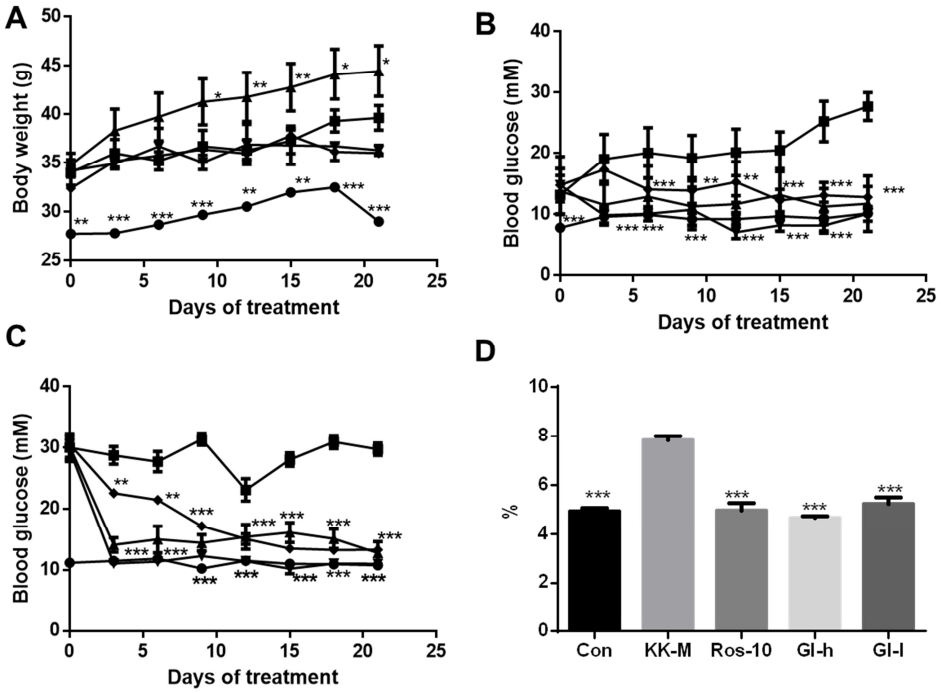

Figure 6. Effects of ganomycin I (**4**) on body weight and blood glucose levels. (A) Body weight in KK-A^y mice, (B) Sequential monitoring of blood glucose in KK-A^y mice after 4h fasting, (C) Free diet blood glucose in KK-A^y mice, (D) HbA1c in KK-A^y mice. Values are means ±SEM (n = 8 for KK-A^y mice); **P*<0.05, ***P*<0.01, ****P*<0.001 versus KK-A^y model group. Con, ●, C57BL/6J mice control; KK-M, ■,KK-A^y model; Ros-10, ▲, rosiglitazone 10 mg/kg; GI-h, ⊖ ganomycin I (**4**) 5 mg/kg; GI-l, ▲ GI-l 1 mg/kg.

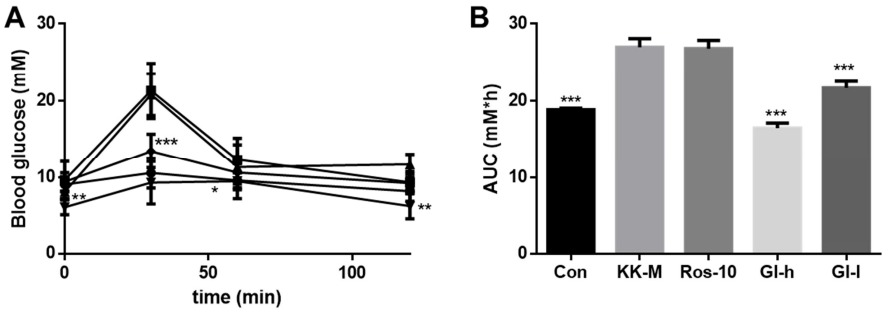

Figure 7. Effects of ganomycin I (**4**) on oral sucrose tolerance test (OSTT). (A) OSTT and (B) AUC of the OSTT on the 20th day of treatment in KK-A^y mice. Values are means ±SEM. (n = 8 for KK-A^y mice); **P*<0.05, ***P*<0.01, ****P*<0.001 versus KK-A^y model group. Con, ⊷, C57BL/6J mice control; KK-M, ⊷,KK-A^y model; Ros-10, ⊷, rosiglitazone 10 mg/kg; GI-h, ⊷ ganomycin I (**4**) 5 mg/kg; GI-l, ⊷ GI-l 1 mg/kg.

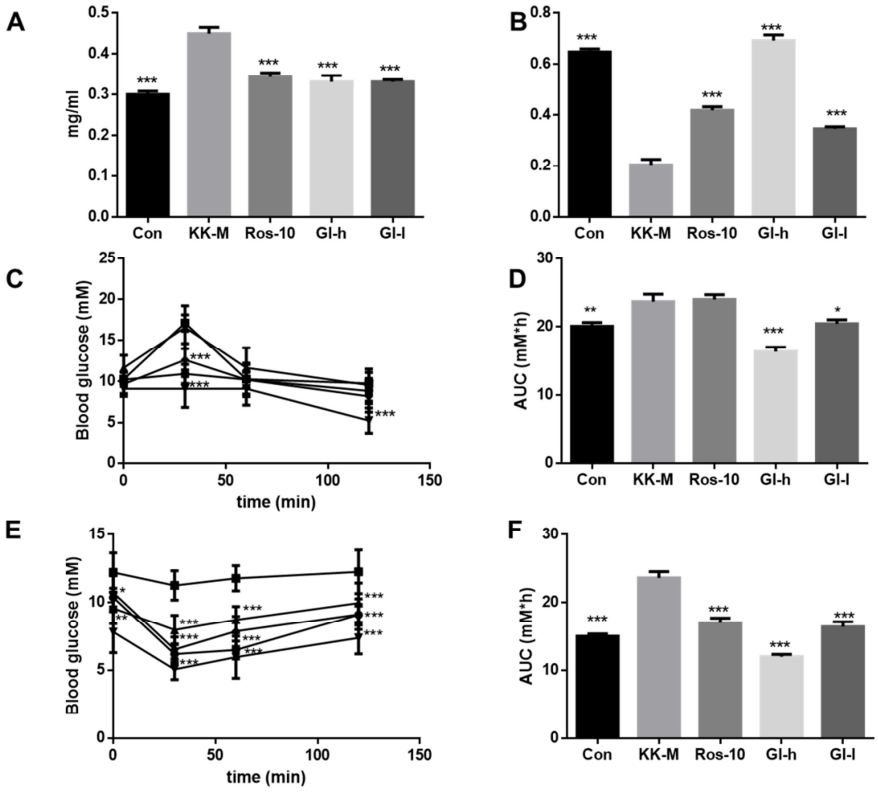

Figure 8. Effects of ganomycin I (**4**) on insulin resistance. (A) Serum insulin in KK-A^y mice, (B) ISI in KK-A^y mice, (C) OGTT and (D) AUC of OGTT on the 21th day of treatment in KK-A^y mice. (E) ITT and (F) AUC of the ITT on the 19th day of treatment in KK-A^y mice. Values are means ±SEM (n = 8 for KK-A^y mice); **P*<0.05, ***P*<0.01, ****P*<0.001versus KK-A^y model group. Con, ●, C57BL/6J mice control; KK-M, ■,KK-A^y model; Ros-10, ▲, rosiglitazone 10 mg/kg; GI-h, ⊖ ganomycin I (**4**) 5 mg/kg; GI-l, ▲ GI-l 1 mg/kg.

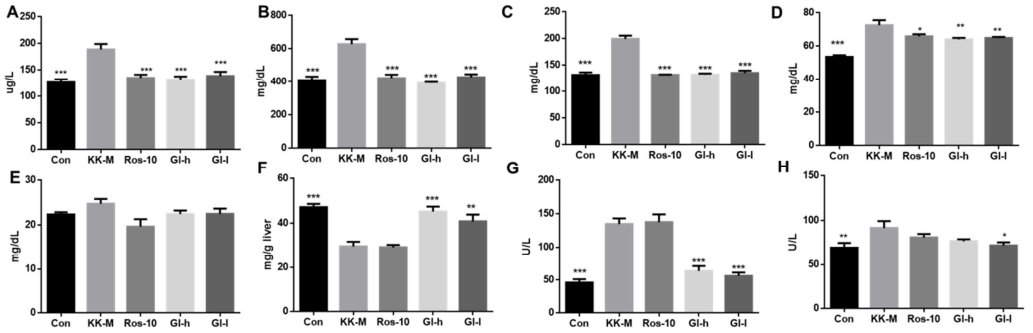

Figure 9. Effects of ganomycin I (**4**) on AST, ALT, blood lipids. (A) Serum NEFA in KK-A^y mice, (B) Serum TG in KK-A^y mice (C) Serum TC in KK-A^y mice and (D) Serum LDL-C in KK-A^y mice, (E) Serum HDL-C in KK-A^y mice, (F) liver hepatic glycogen in KK-A^y mice (G) Serum AST in KK-A^y mice, (H)Serum ALT in KK-A^y mice. Values are mean ±SEM (n = 7-8 for KK-A^y mice); **P*<0.05, ***P*<0.01, ****P*<0.001 versus KK-A^y model group. Con, C57BL/6J mice control; KK-M, KK-A^y model; Ros-10, rosiglitazone 10 mg/kg; GI-h, ganomycin I (**4**) 5 mg/kg; GI-l, GI-l 1 mg/kg.

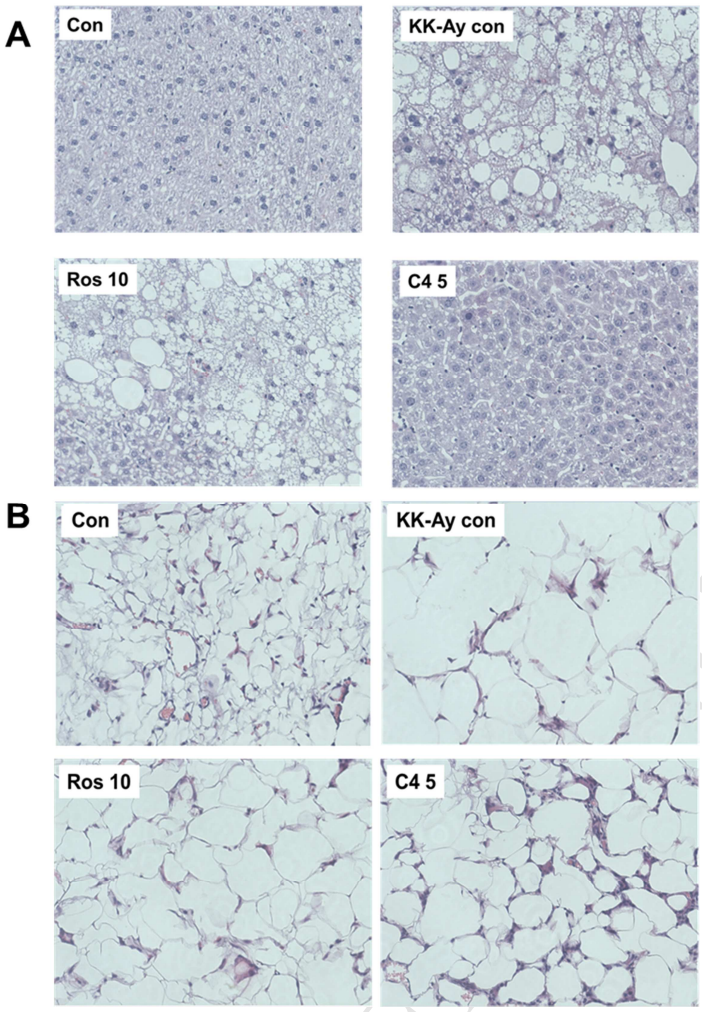

Figure 10. Photomicrographs of liver, WAT sections of the KK-A^y mice treated with ganomycin I (**4**). (A) Liver. Hypertrophy of hepatocytes and hepatic steatosis are evident. (B) WAT. (HE: 20×). Con, C57BL/6J mice control; KK-M, KK-A^y model; Ros-10, rosiglitazone 10 mg/kg; GI-h, ganomycin I (**4**) 5 mg/kg;

Table 1. ^{1}H and ^{13}C NMR data of **1-3** (in $CDCl_3$)

No.	**1**		**2**		**3**	
	δ_H (m, *J* in Hz)	δc	δ_H (m, *J* in Hz)	δc	δ_H (m, *J* in Hz)	δc
1	3.67 (dd,15.9， 7.3) 3.81 (dd, 15.9， 7.3)	28.6	3.49 (d, 7.4)	29.5	6.17 (s)	78.2
2	6.19 (t, 7.3)	141.4	7.01 (t, 7.4)	142.6	7.23 (s)	148.3
3		131.3		132.3		132.7
4	2.46 (m);2.63 (m)	32.8	2.44 (t, 7.6)	26.9	2.37 (t, 7.2)	25.4
5	2.32 (m)	25.4	2.17 (td, 14.8, 7.6)	27.6	2.30 (m)	25.9
6	5.14 (t, 7.2)	126.0	5.18 (t, 7.0)	123.3	5.13 (t, 6.5)	124.0
7		134.9		136.4		135.3
8	2.34 (m);2.01 (m)	35.8	1.97 (t, 7.0)	39.8	2.17 (t, 7.2)	37.9
9	1.48 (m)	27.8	2.06 (td, 14.7, 7.0)	26.8	2.42 (m)	27.3
10	3.73 (t, 9.0)	71.4	5.09 (t, 7.0)	124.5	6.45 (t, 6.7)	155.2
11		83.0		131.6		139.5
12	1.05 (s)	22.9	1.67 (s)	25.8	1.74 (s)	9.4
13	1.34 (s)	22.2	1.59 (s)	17.8		196.0
14	1.52 (s)	15.5	1.59 (s)	16.2	1.61 (s)	16.2
15		171.0		172.2		174.5
16		126.5		126.6		123.2
17		149.1		149.7		150.2
18	6.72 (d, 8.8)	116.3	6.63 (d, 8.4)	117.0	6.69 (s)	117.0
19	6.75 (dd, 8.8, 2.9))	123.0	6.59 (s)	116.4	6.69 (s)	116.4
20		147.7		147.5		146.6
21	6.87 (d, 2.9)	124.3	6.58 (s)	114.3	6.64 (s)	112.6

Table 2. HMG-CoA reductase and α-Glucosidase inhibitory activity of **1-8**

	HMG-CoA reductase inhibition (IC_{50}, μM)	α-glucosidase inhibition (from Baker's yeast) (IC_{50}, μM)	Small intestinal mucosa from rat		
			α-glucosidase inhibition (IC_{50}, μM)	sucrase inhibition (IC_{50}, μM)	maltase inhibition (IC_{50}, μM)
1	>100	6.3±1.1	3.6±0.6	>100	45.8±8.1
2	>100	>100	>100	>100	>100
3	>100	12.7±2.1	15.8±2.2	>100	80.1±10.3
4	12.3±1.7	0.3±0.1	0.4±0.1	67.6±10.2	3.6±0.3
5	29.3±2.5	1.6±0.2	5.9±0.5	35.5±6.5	17.8±4.7
6	>100	32.1±5.2	61.2±10.2	>100	46.2±12.3
7	56.9±12.1	10.2±2.3	15.8±2.3	>100	23.8±5.9
8	45.2±7.1	3.2±0.7	6.4±0.8	>100	18.1±2.9
Positive control	Atorvastatin 32.1±7.7	Acarbose 273.1±30.5	Acarbose 38.1±6.0	Acarbose 20.2±4.5	Acarbose 16.1±4.1

Graphical abstract

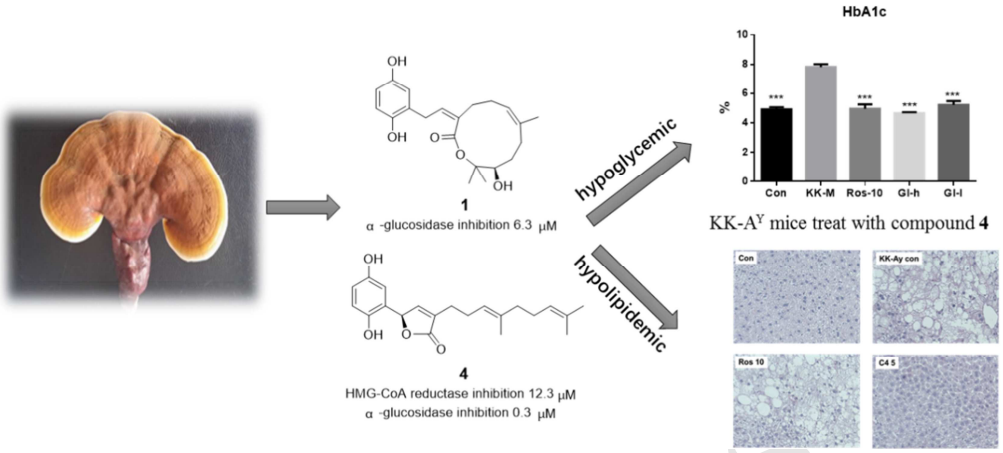

Highlights

- Three new meroterpenoids, together with five known meroterpenoids, were isolated from the fruiting bodies of *Ganoderma leucocontextum*.
- The inhibitory effects of **1**-**8** on HMG-CoA reductase and α-glucosidase were tested *in vitro*.
- Docking studies of compound **4** into *α*-glucosidase.
- Ganomycin I (**4**) exerted potent and efficacious hypoglycemic, hypolipidemic, and insulin-sensitizing effects in KK-A^y mice.